ELSEVIER

Teaser Carbon dots show significant potential as theranostics for the improved management and treatment of cancer.

Carbon dots: emerging theranostic nanoarchitectures

Vijay Mishra[1], **Akshay Patil**[1], **Sourav Thakur**[2] and **Prashant Kesharwani**[3,‡]

[1] Department of Pharmaceutics, Lovely Institute of Technology (Pharmacy), Lovely Professional University, Phagwara, Punjab 144411, India
[2] Department of Quality Assurance, Lovely Institute of Technology (Pharmacy), Lovely Professional University, Phagwara, Punjab 144411, India
[3] School of Pharmacy, Department of Pharmaceutical Technology, International Medical University, Jalan Jalil Perkasa 19, Kuala Lumpur 57000, Malaysia

Nanotechnology has gained significant interest from biomedical and analytical researchers in recent years. Carbon dots (C-dots), a new member of the carbon nanomaterial family, are spherical, nontoxic, biocompatible, and discrete particles less than 10 nm in diameter. Research interest has focused on C-dots because of their ultra-compact nanosize, favorable biocompatibility, outstanding photoluminescence, superior electron transfer ability, and versatile surface engineering properties. C-dots show significant potential for use in cellular imaging, biosensing, targeted drug delivery, and other biomedical applications. Here we discuss C-dots, in terms of their physicochemical properties, fabrication techniques, toxicity issues, surface engineering and biomedical potential in drug delivery, targeting as well as bioimaging.

Introduction

Nanotechnology has gained significant interest from biomedical and analytical researchers in recent years. Nanoparticles (NPs), as a result of their florescent properties, show potential for use in biosensing, chemical sensing, imaging, and biological monitoring [1]. There is an emerging focus on developing new nontoxic nanocarriers. C-dots are discrete, spherical particles less than 10 nm in diameter. They have a sp^2 hybridized structure that includes oxygen in the form of various oxygen-containing species, such as hydroxyl (–OH), carboxyl (–COOH), and aldehyde (–CHO) groups. C-dots also comprise well-organized carbon atoms with a high aspect ratio, large surface area, high thermal and chemical stabilities, and a significantly higher drug-loading capacity compared with larger particles, such as quantum dots (Q-dots) [2]. The properties of C-dots include excellent water solubility, biocompatibility, good conductivity, photochemical

Corresponding authors: Mishra, V. (vijay.20352@lpu.co.in), Kesharwani, P. (prashantdops@gmail.com), (prashant_pharmacy04@rediffmail.com)
‡ Present address: Pharmaceutics and Pharmacokinetics Division, CSIR-Central Drug Research Institute, Lucknow, 226031, U.P., India.

Vijay Mishra is an associate professor of pharmaceutics at Lovely Institute of Technology (LIT; Pharmacy), Lovely Professional University, Phagwara, (Punjab), India. Dr Mishra earned his PhD from Department of Pharmaceutical Sciences, Dr H.S. Gour Central University, Sagar (MP), India. He has been a recipient of several internationally acclaimed fellowships and awards, including Graduate Research Fellowship (AICTE, New Delhi), UGC-BSR Senior Research Fellowship (UGC, New Delhi) and an International Travel Award/Grant (ICMR, New Delhi). He has authored, co-authored, and/or edited more than 28 papers, two book chapters, and books. He serves as a reviewer for, and an editorial board member of various journals. His current research interests encompass siRNA delivery, surface-engineered dendrimers, carbon nanotubes, carbon dots, quantum dots, and gold nanoparticle-based drug delivery systems.

Akshay Patil is currently studying for a MPharm at LIT under the guidance of Vijay Mishra. His current research interests include dendrimers, carbon nanotubes, carbon dots, and novel drug delivery systems.

Sourav Thakur is currently studying for a MPharm at LIT. His research interests include quality control in drug delivery systems, quality by design, risk management, and artificial intelligence.

https://doi.org/10.1016/j.drudis.2018.01.006

Prashant Kesharwani is currently working as a Ramanujan Fellow at Central Drug Research Institute (CDRI), Lucknow, India. He received his PhD in pharmaceutical sciences from the Dr H.S. Gour University (Sagar, India) within the group of N.K. Jain. He is a recipient of several internationally acclaimed awards, including a Ramanujan Fellowship, DST, India (2017), Excellence Research Award (2014), Young Innovator Award (Gold medal; 2012), International Travel Award/Grant from DST (New Delhi), and INSA (CCSTDS, Chennai) (2012). He received a ICMR Senior Research Fellowship (for his PhD) and an AICTE Junior Research Fellowship (for his MPharm.). After his doctorate, he worked as a postdoctoral fellow in Wayne State University in Detroit (Michigan, USA). Dr Kesharwani subsequently joined the School of Pharmacy, International Medical University (Malaysia) as a lecturer in pharmaceutical technology. An overarching goal of his current research is the development of nano-engineered drug delivery systems for cancer with a focus on dendrimer-mediated drug delivery systems. Dr Kesharwani is a co-author of more than 85 publications in international journals and two international books.

stability, low toxicity, and environmental friendliness [3]. Thus, there have been a significant number of protocols developed for the fabrication of C-dots, involving both natural and synthetic precursor strategies. The former includes natural precursors, such as glucose [4], sugar, jaggery, and bread [5], grass [6], egg [7], soya milk [8], beverages such as Kvass, beer, and malta, [9], orange juice [10], glycerol [11], *Bombyx mori* silk [12], amino acids [13], *N*-acetyl cysteine [14], banana juice [15], citric acid [16], sucrose [17], Chinese ink [18], instant coffee [19], potato [20], beer [21], solid biomass, such as chicken eggs, orange juice with ethanol, coffee grounds, bee pollen, and oleic acid [22], and algal blooms [23], whereas synthetic methods include arc discharge [24], ultrasonic/microwaves [25], laser ablation [26], electrochemical synthesis [27], and hydrothermal treatments [16]. C-dots with different structure-specific properties can also be fabricated by surface engineering, illustrating their excitation-independent and -dependent properties [28].

The toxicological nature of a nanomaterial has an important role in understanding its mode of action. Toxicological properties have a role in inflammation, carcinogenesis and various other pathological processes [29]. For example, Q-dots attracted the attention of researchers because of their size-dependent optoelectrical properties, which are used in photovoltaics, sensors, and imaging. However, the core toxicity showed by Q-dots limits their biological application. Thus, there was a drive to develop a non-toxic Q-dot-like nanomaterial: C-dots. Given their superior water dispersibility resulting from the presence of –OH or –COOH groups, C-dots also exhibit strong fluorescence in the infrared (IR) and visible regions, as well as physicochemical and photochemical stability. A comparison of C-dots with other carbon-based nanomaterials, such as carbon nanotubes (CNTs) and graphene, is provided in Table 1.

Targeted drug delivery is one of the prominent properties of C-dots. Previously, traditional drug carrier moieties were hard to trace and/or observe. However, research showed that a fluorescent C-dot core combined with a drug moiety resulted in an excellent drug delivery tool. In addition, the combined effect of one or more functional groups incorporated on the surface of C-dots has resulted in a useful tool for the treatment of disease [2]. C-dots can also be applied for the delivery of anticancer drugs. Conventional chemotherapy can eliminate and reduce tumors but with the adverse effect of damaging healthy tissue. This can be overcome by targeted drug delivery using nontoxic C-dots [30,31].

As an alternative to Q-dots, C-dots show low cytotoxicity and good photostability; thus, they have been used extensively in diagnostic imaging. At a specific dot level, C-dots show high brightness, detectable emission wavelengths, and visible excitation [32]. Here, we describe recent progress in the use of C-dots, highlighting their potential for targeted drug delivery and diagnostic imaging.

Historical background of carbon dots

During the 1980s, carbon filaments were fabricated with a diameter of less than 10 nm, although few studies were performed with them at the time. The first systematic study of carbon filaments was performed following the discovery of fullerenes by Smalley *et al*. [33]. Carbon occurs in several nanoforms in addition to fullerenes and, thus, fluorescent carbon nanomaterials are the newest member of the carbon NP family [34].

C-dots were accidently discovered by Xu *et al*. in 2004 following the observation of fluorescence during the separation of single-walled CNTs (SWCNTs) using gel electrophoresis from carbon soot produced by arc discharge [24]. Based on this study, in 2006, Sun *et al*. synthesized fluorocarbon NPs less than 10 nm in diameter, naming them C-dots [35]. During their initial development, C-dots were manufactured from natural, biological sources of carbon; however, following modification, C-dots began to be

TABLE 1

Comparison of C-dots and other carbon-based nanomaterials

Nanomaterial	Characteristics	Applications	Limitations	Refs
Graphene	Comprises one atom-thick carbon (sp^2 hybridized) sheets of six-member rings, providing an exposed surface area that is nearly twice as large as that of SWCNTs	High mechanical strength, high elasticity, thermal conductivity	Absence of metallic impurities that can affect accuracy of sensor; commercial availability of graphene and graphene platelets is limited	[20,54]
CNTs	Unique combination of stiffness, strength, and tenacity compared with other fiber materials; high thermal and electrical conductivity	Can reach cytoplasm and nucleus through the lipid bilayer, thus have potential use in biosensors, biomedical devices, and drug delivery; greater ability of conjugation with various bioactive agents, such as peptides, proteins, nucleic acids, and therapeutic agents; greatest stability of nanocarriers	Severe toxicity in cultured cells, such as human keratinocytes, T lymphocytes, kidney cells, alveolar macrophages, and endothelial cells *in vitro*; reproduce cellular oxidative stresses, thus incompatible with biological systems; insoluble in most common solvents	[29,34]
C-dots	Zero-dimensional nanocarriers with diameter <10 nm; spherical nanocrystal design; synchronized sp^2 and sp^3 hybridization	Used for targeted drug and gene delivery, tumor targeting, monitoring of cellular trafficking, and diagnostic imaging	Poor stability; difficult to maintain properties for long periods of time	[36,57,74]

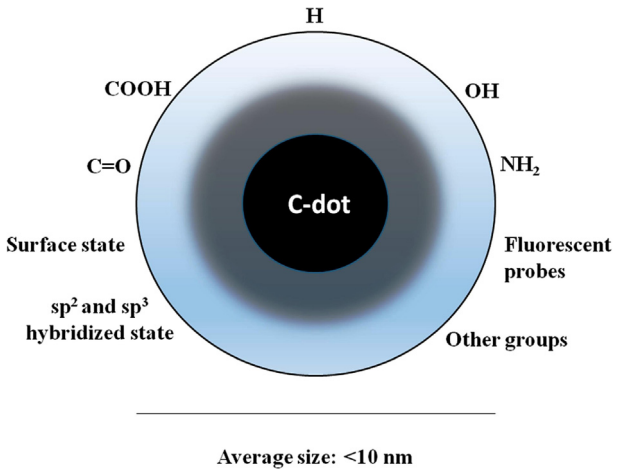

FIGURE 1

Design of carbon dots (C-dots) with different surface functional groups.

fabricated using synthetic carbon probes. Extensive research has been done on the fabrication, characterization, drug delivery, and bioimaging of C-dots. Their significant properties include their inert chemical and biocompatible nature, simple functionalization, photoluminescence, low toxicity, and resistance to photobleaching. This has made C-dots a focus in the fields of biosensing, bioimaging, optoelectronics, drug delivery, and photovoltaics.

Design of carbon dots

C-dots are zero-dimensional nanocarriers with a diameter of less than 10 nm (Fig. 1). High-resolution transmission electron microscopy (HR-TEM) imaging and atomic force microscopy (AFM) imaging reveal the spherical nanocrystal design of C-dots [36]. C-dots generally have a well-ordered spherical shape with –OH, –COOH, and $–NH_2$ (amine) groups on their surface, which provide them with high biological activity, excellent water solubility, and their ability to form conjugates with various inorganic and organic substances [37]. There are currently two types of C-dot: amorphous-based C-dots (A-C-dots) and graphene-Q-dots (G-Q-dots). A-C-dots are formed by the synchronized sp^2 and sp^3 hybridization of carbon probes, with the ability to surface engineer these molecules further. G-Q-dots have a sp^2-hybridized nanocrystalline carbon core, an asymmetrical configuration that results from the large number of N and O moieties that interrupt the carbonic framework [21].

Properties of carbon dots

C-dots have various fascinating properties (Fig. 2), as discussed in this section.

Absorption

Strong optical absorption has been shown by C-dots in the ultraviolet (UV) region (mainly 280–360 nm). Surface modifications can regulate the absorption band of C-dots, and the emission properties of C-dots generally depend upon the level of excitation [20]. Surface functional moieties have an important role in determining the absorption ranges of C-dots. Following surface passivation with polyethyleneimine (PEI), Liu and co-workers reported red (330–355 nm), blue (460–495 nm) or green (530–550 nm) luminescence. The nonuniformity of PEI passivation on C-dots disrupts the photoluminescence and, thus, excitation occurs at longer wavelengths [38]. C-dots show optical absorption in the UV region and some traces of absorption in the visible region. Top-down fabricated C-dots show size-dependent absorption from 200

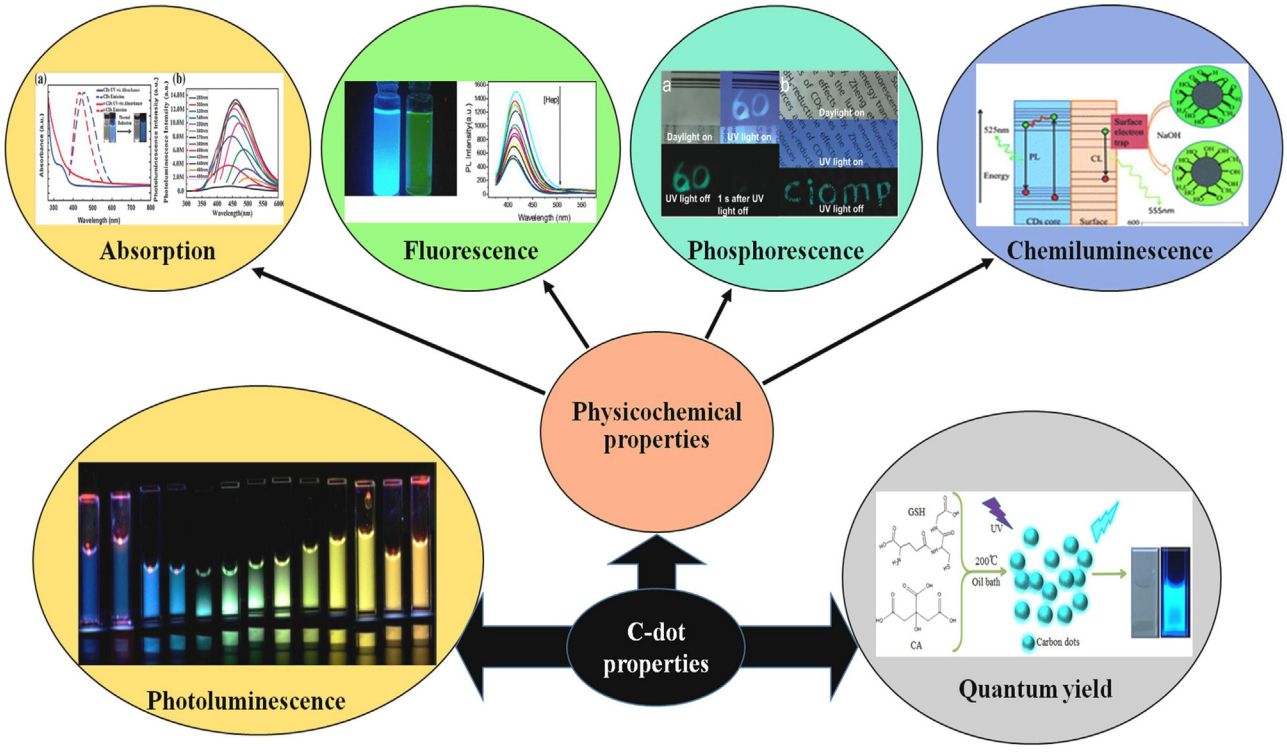

FIGURE 2

Properties of carbon dots (C-dots).

to 252 nm (6.20–4.92 eV) with an increase in diameter from 12 to 22 nm. However, C-dots fabricated from the same material but using different fabrication techniques, such as microwave, ultrasonic, and hydrothermal approaches, show different absorption bands, within the 250–300-nm range [39].

Fluorescence

C-dots show high fluorescent effects and are being developed as fluorescent molecules because of their excellent biocompatibility, low photobleaching and protean surfaces for use in biomedicine, sensing, bioimaging and catalysis. Zhang *et al*. reported the strong fluorescent nature of C-dots fabricated from a single-step hydrothermal treatment [40]. Recently, Wang *et al*. reported the highly sensitive nature of C-dots. C-dots prepared using *O*-aminophenol as the starting material displayed bright-green fluorescence with excitation and emission peaks at 420 and 500 nm, respectively, with a quantum yield (QY) of 0.28, and blue fluorescence at 300 and 400 nm, respectively, with a QY 0.40. Amino and hydroxy groups together display novel emission properties and C-dots have been found to be a viable fluorescent probe for heparin [21].

Phosphorescence

The phosphorescence properties of C-dot were highlighted when water-soluble C-dots were used as a phosphorescent material. C-dots mixed with a matrix of polyvinyl alcohol (PVA) showed clear phosphorescence under UV. Aromatic carbonyl groups present on the surface of C-dots provide a triplet excited state, which results in the phosphorescence [3].

Deng *et al*. reported the phosphorescence properties of a C-dot-based water-soluble phosphorescent material [41]. At room temperature, clear phosphorescence of PVA-dissolved C-dots was detected. Triple excited states of carbonyls present on the surfaces of the C-dots were found to result in the phosphorescence. As a result of the solidification process, the PVA matrix shields the triplet excited state energy following the formation of hydrogen bonds [41].

Chemiluminescence

The chemiluminescence of C-dots is exploited for the determination of radioactive substances. The chemiluminescent intensity depends exclusively on the concentration of C-dots within a certain absorption range. For example, Lin *et al*. mixed C-dots with oxidants, including cerium and potassium permanganate ($KMNO_4$), resulting in the chemiluminescence of the C-dots [42]. By contrast, Zhao *et al*. reported the excellent electron-donating capability of C-dots towards dissolved oxygen to form superoxide anion radicals (O_2^-) in strong alkali solutions, such as NaOH or KOH, resulting in chemiluminescence [43].

Photoluminescence

Photoluminescence (PL) is one of the most-outstanding features of C-dots. Although much work has focused on finding the source of the PL of C-dots, this remains an issue of debate. The key points to the PL properties of C-dots are a diameter of <10 nm and a zero-dimensional structure. Thus, the morphology, composition, size, and crystalline nature of C-dots affect their PL nature. These features are determined by the initial precursors and fabrication techniques used to form the C-dots [32]. Liao *et al*. reported the enhanced PL properties of spiropyran-functionalized C-dots achieved via surface modulation [44]. Recently, Jiang *et al*. reported a new, simple fabrication strategy for C-dots involving exposure to a single UV light, given that C-dots emit blue, green, and red (BGR) light [45]. Xu *et al*. fabricated highly PL C-dots from graphene nanofibres doped with sulfur for the detection of Fe^{3+} ions and revealed the charge-dependent emission nature of these C-dots. The charge-separated C-dots under 365-nm UV light emitted different colors [20].

Recently, Wang *et al*. fabricated highly PL, nitrogen-doped C-dots using a one-step hydrothermal treatment with m-aminobenzoic acid as precursor for the detection of iron ions. The charge density of the C-dots changed according to their electron richness, resulting in the transfer of energy to an excited π^* state. Large amounts of energy were released because of the transformation of π^* to π, leading to higher QY. The authors reported the strongest peak of PL at 415 nm [46].

Quantum yield

For a luminescent material, QY is an important aspect to take into consideration. The QY of C-dots depends mainly upon the starting material or fabrication method. During their early development, C-dots fabricated from graphite, candle soot, and citric acid reported QY up to 10% [20]. Various approaches, such as surface engineering and element doping, are useful for increasing the QY of C-dots. Although nitrogen and sulfur are mainly used as doping materials, the use of boron has also been reported. The improved QY of C-dots increases nonlinearly with their optical properties [47]. By using citric acid and glutathione as starting materials, Zhuo *et al*. fabricated C-dots with a QY of approximately 80.03% [48].

Advantages and disadvantages of carbon dots

As we discuss below, C-dots have various advantages and disadvantages over other carbon and metallic nanomaterials (Table 2).

Advantages of carbon dots

Their biocompatible nature and inexpensive fabrication techniques render C-dots rising stars in the carbon nanomaterial family. Given their abundant surface groups, C-dots have tendency to bind inorganic and organic molecules. In addition, C-dots engineered by various techniques are useful in bioimaging, chemical sensing, and diagnostic imaging. Given the basic building blocks of C-dots is carbon, they are also associated with low toxicity and their nano size enables *in vivo* cellular entry. Although carbon shows poor solubility in water, C-dots exhibit good water solubility and photoluminescence. C-dots can be administered via various routes, including nasal, oral, parental, and pulmonary means. C-dots fabricated from natural precursors, such as plants and trees, can act as drugs for different diseases. For example, C-dots fabricated from ginger and tea inhibit HeLa, HepG2, MCF-7, and MDA-MB-231 cells [39].

Disadvantages of carbon dots

C-dots show poor stability, with those fabricated using organic material remaining stable for only a few weeks [49]. Thus, it is difficult to control the properties of C-dots longer term. The fabrication techniques used to produce C-dots, such as carbonization and

TABLE 2

Advantages and disadvantages of carbon versus metallic nanomaterials

Nanomaterial	Advantages	Disadvantages	Refs
Fullerenes	Relatively high electron affinity; hydrophobic surface that increases their adsorption capacity towards organic molecules, as well as permeability through lipid membranes	Biodistribution, absorption, lifetime, excretion, and, ultimately, poor consumer safety	[86]
Q-dots	Different optical, electronic, and physical properties; optoelectronic properties change as a function of both size and shape, emission colors at longer wavelengths display distinct quantized energy spectrums, less photobleaching, and brighter images	Inherently toxic; biological behavior of tumors deciphered by engineered fluorescent Q-dot nanoprobes	[1]
Gold NPs	Size- and shape-dependent visual and electronic characteristics, temperature-dependent electron transport properties	Gold is associated with acute or chronic toxicity, weak optical signal, poor tumor-targeting efficiency	[87]
Dendrimers	Highly branched polymeric structure, capable of delivering bioactives, such as genes, vaccines,and various drugs	Large-scale fabrication is not possible; associated toxicity	[88]
C-dots	Good aqueous solubility, biocompatible, inexpensive fabrication techniques; PL properties for use in bioimaging, chemical sensing, and diagnostic imaging	Long-term stability issues in terms of the control of their properties	[36,39,49]

pyrolysis, result in complex molecular structures that can be difficult to interpret using characterization techniques, such as nuclear magnetic resonance (NMR) and IR spectroscopy. The different carbon sources, structures, and surface ligands used in the manufacturing of C-dots also affect their chemical, electrical and optical properties.

Carbon dot fabrication methods

Over the past decade, various techniques have been proposed for the fabrication of C-dots. These techniques fall into two main categories: top-down approaches and bottom-up approaches (Fig. 3). Bottom-up approaches include natural fabrication methods using molecular precursors, including biomass [10,22], eggs [7], coffee grounds [50], pollen bees [22], oleic acid [22], and Chinese ink [18]. Top-down approaches mainly involve synthetic methods of fabrication, including arc discharge [24], chemical ablation [51], laser ablation [35], microwave irradiation [25], and electrochemical carbonization [52] (Table 3).

Bottom-up approach

Bottom-up approaches use various natural carbon sources, as discussed below.

Biomass

Biomass holds great potential for the fabrication of C-dots. Under this method, hydrothermal treatment of ethanol with orange juice at 120 °C for 150 min gave a yield of 0.4 g C-dots. A longer shelf-life and better expedient scalability in mass of precursors make solid biomass a better option than liquid biomass for synthesizing C-dots [10].

Plasma-induced pyrolysis

Chen and co-workers were the first to fabricate 10 g of C-dots by plasma-induced pyrolysis using chicken eggs as a biological carbon source [7].

Using pollen as carbon source

Recently, Zhang and Yu used 10 g of bee pollen as a carbon source to fabricate 3 g of C-dots [22].

Carbonization of sucrose

Besides carbon biomass, molecular precursors can be used directly to fabricate C-dots on a gram-scale level. Chen *et al*. obtained a high yield (approximately 41.8%) using a simple fabrication technique. The authors heated 20 g of sucrose in oleic acid at 215 °C for 5 min with vigorous stirring under N_2 protection, followed by supernatant purification to yield 8.36 g of C-dots [14]. Bhunia and co-workers fabricated C-dots under controllable carbonization at a temperature range of 80–300 °C, using different solvents and desiccating agents [53].

Chinese ink

Using Chinese ink as raw material, Yang *et al*. fabricated 120 g of C-dots in a one-pot fabrication method. Carbon materials are ideal precursors for the macroscale fabrication of C-dots; however, the large quantity of strong acids that are liberated can cause environmental pollution [18].

Eutrophic algal blooms

Recently, Vadivel *et al*. used eutrophic algal blooms as a starting material to fabricate C-dots of approximately 8 nm diameter with a QY of 13%. These naturally fabricated C-dots were reported to have excellent cell permeability, high photostability, and luminescence stability under different atmospheric conditions [23].

Top-down approach

Arc discharge method

Xu *et al*. observed fluorescent NPs from SWCNTs by arc discharge. The SWCNTs were functionalized by fumes of nitric acid (HNO_3). The precipitate was extracted out by NaOH (pH 8.4) and C-dots present in the precipitate were separated using gel electrophoresis. A fluorescence QY of 1.6% was reported for these C-dots, which showed green, yellow, and orange fluorescence. Elemental analysis revealed the presence of carbon (53.93%), oxygen (40.33%), hydrogen (2.6%), and nitrogen (1.20%) [24].

Chemical ablation

In this method, a strong oxidizing agent transforms small organic precursors into carbonaceous material. Amino-terminated C-dots were fabricated by dehydration in aqueous solution with concentrated H_2SO_4 followed by further breakdown of the carbon nanoprecursor to form C-dots with HNO_3 and surface engineering with 4,7,10-trioxa-1, 13-tridecanediamine [51].

Dong *et al*. extracted electrochemiluminescent C-dots from activated carbon by chemical ablation. In addition to excellent

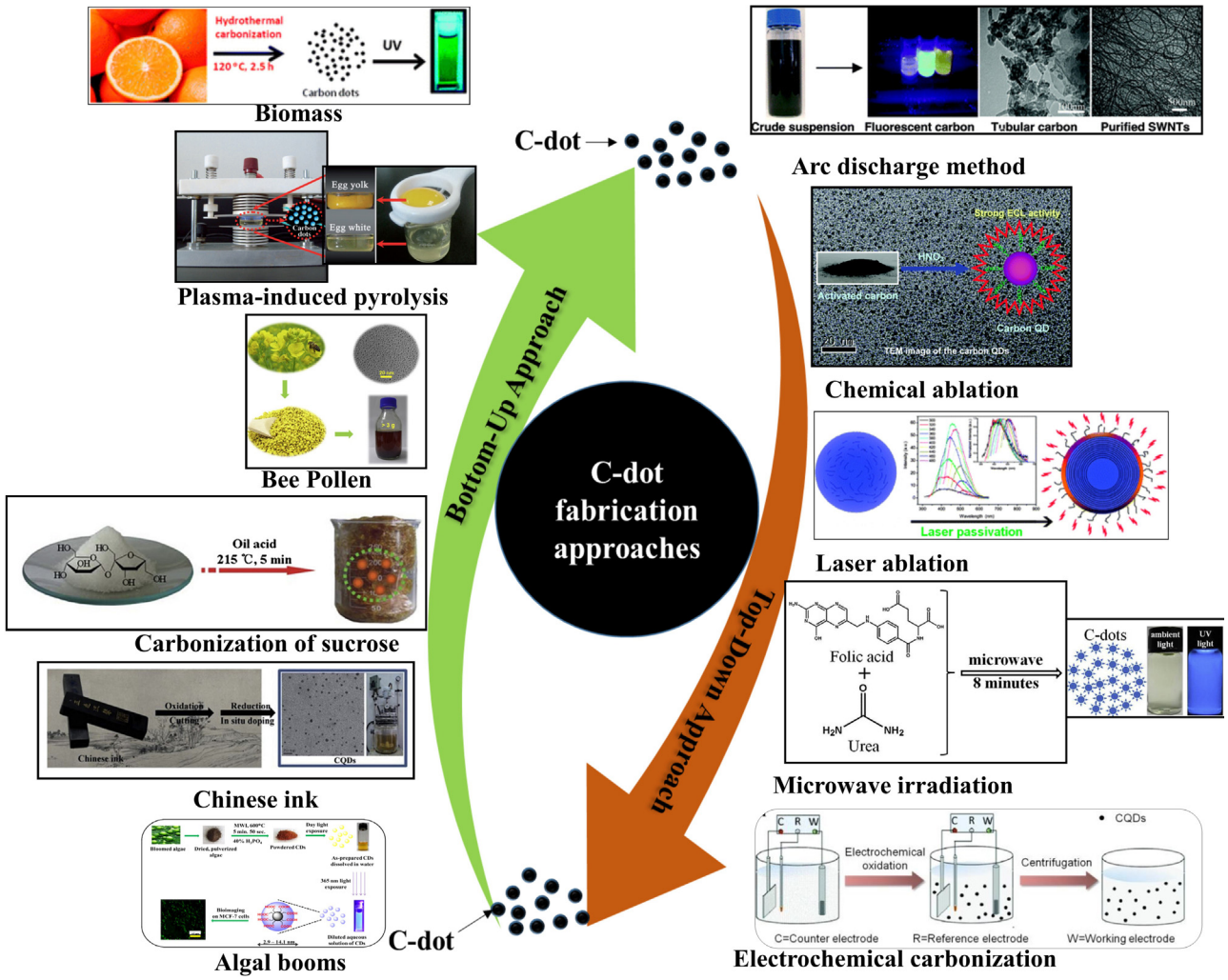

FIGURE 3

Carbon dot (C-dot) fabrication strategies.

electrochemiluminescent activity, the authors obtained C-dots of 3–4 nm diameter with a QY > 10%, which suggested the use of these C-dots for large-scale production and biosensing applications [54].

Laser ablation

Sun *et al.*, the pioneers of the laser ablation method, used argon as carrier gas for C-dot fabrication. The desired carbon was obtained from an exhaust cement mixture and graphite powder. A Q-switched Nd:YAG laser (10 464 nm, 10 H_z) was used and the process was carried out at 900 °C and 75 kPa. After ablation, the sample was refluxed with HNO_3 for 12 h and subsequently passivated with polyethylene glycol 1500N (PEG 1500N). The resulted solution was cooled and centrifuged to obtain C-dots of <5 nm [35].

Li *et al.* also fabricated C-dots via a laser ablation technique by taking 0.02 g of carbon nanomaterial dissolved in 50 ml solvent (e.g., water, acetone, or ethanol). The researchers used an Nd:YAG pulsed laser (Spectra-Physics, Santa Clara, USA) with a repetition rate, pulse width, beam diameter, and second

TABLE 3

Advantages and disadvantages of the different methods of C-dot fabrication

Fabrication method	Advantages	Disadvantages	Refs
Arc discharge method	Fabricate NPs in a variety of gases	Requires further purification of C-dots because of coexistence with unwanted carbon material	[24]
Chemical ablation	Various starting materials; most-accessible method	Variable sizes, drastic processes, harsh conditions	[51,54]
Laser ablation	Tunable surface states, rapid process, effective	Low QY, poor control of size	[35]
Microware irradiation	Rapid process, cost effective, ecofriendly	Poor control of size	[25,55]
Electrochemical carbonization	Cost effective, high QY, good control over fabrication technique	Few small-molecule precursors	[52]

'Drastic processes and harsh conditions' reflect the conditions required for chemical ablation like strong oxidizing acids (H_2SO_4 and HNO_3) and controlled oxidation.

harmonic wavelength of 30 Hz, 8 ns, 8 mm, and 532 nm, respectively. The suspension was not irradiated. C-dots were obtained after centrifugation [26].

Microwave irradiation

This is a rapid, ecofriendly, and economic method of C-dot fabrication. Zhu *et al*. fabricated electrochemiluminescent carbon NPs using microwave irradiation. A colorless solution containing glucose and PEG 200 in ultrapure water was subjected to microwave irradiation. Depending on the irradiation time, the solution showed color changes from yellow to dark brown and exhibited variable size and photoluminescence properties [25].

Upon microwave irradiation of a transparent solution of 1,2-ethylenediamine (EDA) and citric acid, Du *et al*. fabricated C-dots showing λ_{ex}-dependent emission behavior [55]. In another study, Liu *et al*., under microwave irradiation, fabricated quasispherical C-dots with an average diameter of 5 nm. Using sucrose as a carbon precursor in diethylene glycol (DEG), the C-dots showed green luminescence at 360 nm within 1 min [56].

Zhang *et al*. fabricated N-doped C-dots from diamonium hydrogen citrate by microwave irradiation for cellular imaging and iron (III) detection. The authors reported 26% QY, which was more than achieved with previously reported microwave irradiation techniques. Moreover, C-dots exhibited favorable biocompatibility and low cytotoxicity, making them a potential tool for the sensitive detection of iron (III) [57].

Electrochemical carbonization

This technique involves the fabrication of C-dots from a bulk carbon source. Zhou *et al*. fabricated C-dots from multiwalled CNTs (MWCNTs) using three electrodes: a working electrode, drawn out from MWCNTs; a counterelectrode (platinum wire); and a reference electrode ($Ag/AgClO_4$). Tetrabutylammonium perchlorate (TBAP; 0.1 M) in acetonitrile was used as the supporting electrolyte solution. During the reaction, the electrolyte solution changed from yellow to dark brown at a potential of −0.2 to 2.0 V and a scanning rate of 500 mV/s. Traces of acetonitrile from C-dots were removed by further evaporation [52].

In another experiment, Ming *et al*. fabricated water-soluble, photocatalytic, and photoluminescent C-dots of high purity and quality using ultrapure water as the electrolyte in the reaction medium [58]. Deng *et al*. fabricated C-dots by electrochemical carbonization of low-molecular-weight alcohols [59], while Liu *et al*. fabricated C-dots with high crystallinity by electrochemical oxidation of a graphite electrode in alkali alcohol. The colorless dispersion of C-dots changed to bright yellow because of the oxygenation of the surface species, demonstrating the effect of pH and the applied potential of C-dots [28].

Surface engineering of carbon dots

Good water solubility, prominent photostability, and low photobleaching render C-dots an effective alternative to Q-dots. Surface engineering involves surface passivation by active functional moieties via different bonds such as covalent, hydrogen, and ionic bonds. Surface-engineered C-dots aid accurate drug delivery, diagnostic imaging, and target-modulated sensing [28].

Yang *et al*. accomplished diagnostic imaging in mice by using surface-engineered PEG 1500N C-dots. Luminescence of surface-engineered PEG1500-C-dots and Q-dots were compared. The green luminescence exhibited by PEG1500-C-dots was comparatively brighter than that emitted by Q-dots. After 6 h of intravenous exposure of surface-engineered C-dots, fluorescence was observed in liver and spleen of mice at 800 nm excitation, with negligible fluorescence in other organs [30].

For dual-fluorescent sensing of copper ions (Cu^{2+}), Zhu and co-workers synergized *N*-(2-aminoethyl)-*N*,*N*,*N*′-tris(pyridin-2-ylmethyl)ethane-1,2-diamine (AE-TPEA-C-dots) and cadmium selenide (CdSe)/Zinc sulfide (Zns)-Q-dots (Fig. 4a) and observed particle residue in various intracellular spaces at physiological pH [8].

Moreover, Kong *et al*. designed surface-engineered C-dots for diagnostic imaging of living cells and tissues at physiological pH. *In vivo* sensing of pH alteration showed good linearity of fluorescent intensity between a pH range of 6.0–8.5. Based on Na^+–K^+ exchange, LCC tumor cells and A549 lung cancer cells showed pH variation. Two-photon microscopy showed that the CPY-C-dots probe could be used to efficiently explore pH variation (Fig. 4b) [60].

For in *vivo* imaging in mice, surface-engineered PEG 1500N-C-dots and ZnS-C-dots were synthesized. Diffusion of surface-engineered C-dots occurred 24 h after administration, with slow excitation emission at 470 and 545 nm for C-dots and C-ZnS, respectively. Green fluorescence indicated the passage of Zns-C-dots from the lymph vessel (Fig. 4c). Elimination of C-dots from the body of the mice was indicated by fluorescence in urine 3 h after administration [30].

Several other reports have examined the surface engineering of C-dots. Li and co-workers controlled the excitation-dependent luminescence of C-dots by surface engineering and simple hydrothermal treatment, forming excitation-dependent and excitation-independent luminescent C-dots (Fig. 4d) [61]. Amine-coated C-dots were fabricated by Fan and co-workers by surface engineering in two simple steps. In the first step, –COOH was converted to a $–NH_2$ group in 2% acetic acid solution followed by carbonization of glucose using hydrothermal treatment by heating for 6 h at 180 °C. Furthermore, PEG 1500 N mixed with –COOH-coated C-dots was heated for 12 h at 120 °C to develop amino-coated C-dots with improved surface functionalization [62].

Carbon dot-related toxicity and remedial strategies

The potential of Q-dots and other fluorescent nanoprobes in optical imaging brought them to the attention of researchers. The performance of Q-dots was accelerated by adding a CdSe base and by varying the particle size. Q-dots are used in *in vitro* and *in vivo* optical imaging for better performance [30]. However, core toxicity caused by Q-dots because of their accumulation in tissues and organs at very low concentrations limits their applications. The quest for a nontoxic and biocompatible fluorescent NP ended with the discovery of C-dots comprising C, O, H, S, and N. In addition to enhanced optical imaging quality and drug delivery efficiency, C-dots only affect the target cells, with *in vitro* and *in vivo* studies demonstrating few or nontoxic effects (Table 4).

In vitro *toxicity studies*

The use of C-dots in living cells and tissues remains a critical issue. The biocompatibility of C-dots fabricated from graphite by electrochemical treatment has been observed in a living kidney cell.

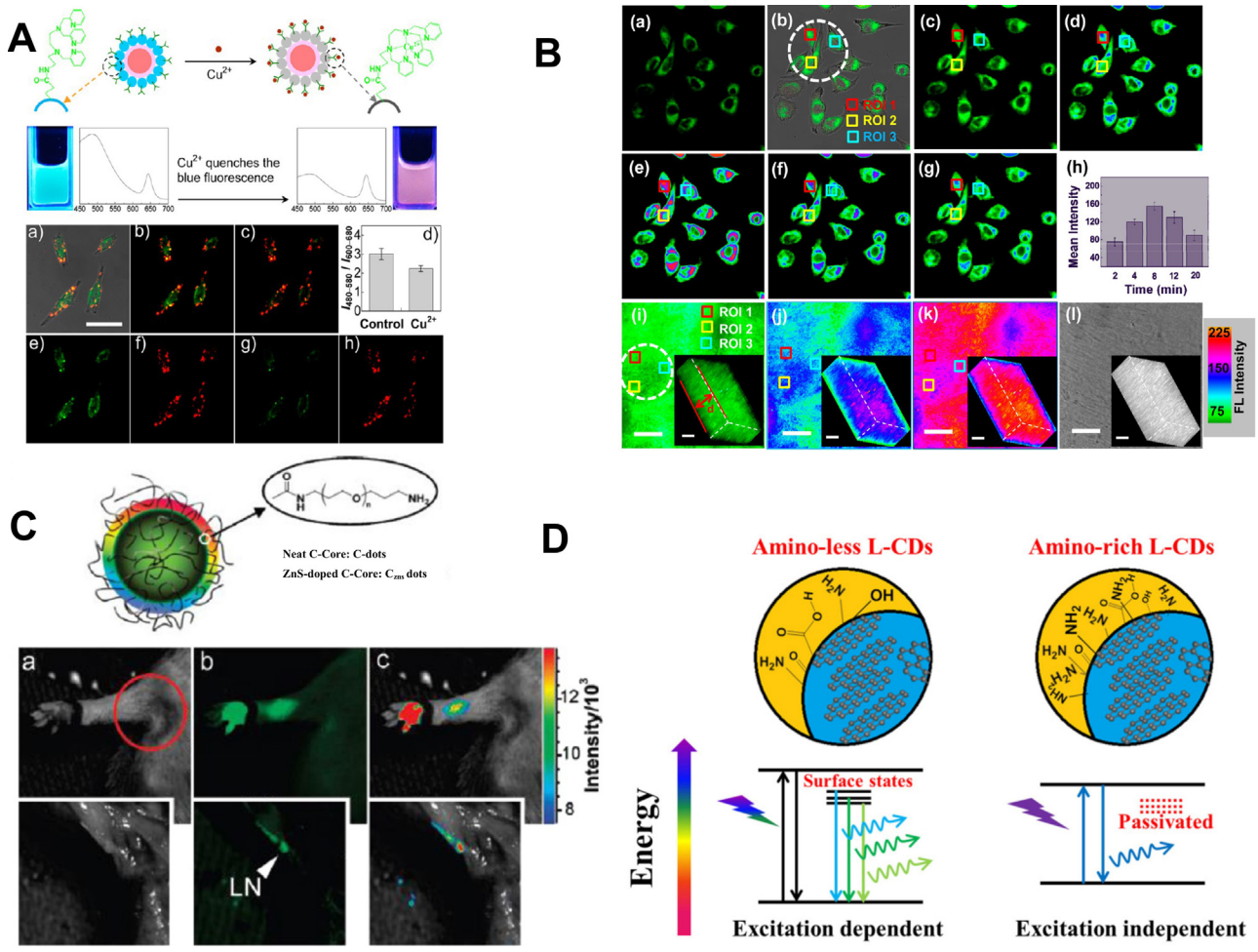

FIGURE 4

Surface engineered carbon dots (C-dots) with imaging properties. (a) CdSe@C-TPEA nanohybrid and overlay of bright-field and fluorescence images of HeLa cells incubated with CdSe@C-TPEA, (b) Na^+–H^+ exchange-dependent two-photon confocal fluorescence images of A549 cells incubated with a C-dot-TPY probe, (c) ZnS-doped C-dots and images post intradermal injection of ZnS-C-dots, and (d) Surface engineering of C-dots with excitation dependent and excitation-independent luminescent properties. Adapted from Refs [8] (a), [60] (b), [30] (c), and [61] (d).

In addition, the results showed that C-dots did not alter cell viability [63].

Yang *et al*. investigated the cytotoxicity and biocompatibility of PEG 1500N surface-engineered C-dots and PEG 1500N as medium in MCF7 (human breast cancer) and HT29 (colorectal adenocarcinoma) cell lines. The results highlighted the viability of the cells post treatment, with lower mortality and cell proliferation in PEG 1500N surface-engineered C-dots-treated cells than in PEG 1500N-treated cells [30].

In an additional study, Fan *et al*. fabricated C-dots with a size range of 2–4 nm via hydrothermal treatment and evaluated their toxicity in a $HepG_2$ cell line. C-dots incubated with cells showed 90% cell viability at a 100 mg ml^{-1} concentration. Cell viability of 49% was observed even at a high concentration of 400 mg ml^{-1} [62].

Initially, there were no reports describing element-based cytotoxicity. The nontoxic assumption of C-dots was proved wrong when Wang *et al*. investigated the toxicity of C-dots on HeLa and MCF 7 cells. The authors fabricated amorphous carbon-based nanodots (ACNDs) by hydrothermal carbonization of polyethylenic amine (PEA) analogs, such as EDA, diethylenetriamine (DETA), and tetraethylenepentamine (TEPA), and citric acid. Bright fluorescence and low cytotoxicity were reported for nitrogen-doped ACNDs in HeLa cells. A cell viability test showed a cell viability of >80% at a high concentration (800 mg ml^{-1}) of ACNDs. Confocal fluorescence microscopy images of HeLa cells were observed under bright-field, blue, green, red, and merged channels by incubating cells with 200 mg ml^{-1} of different ACNDs, such as CD-EDA ($_{2/1}$), CD-DETA ($_{2/1}$), and CD-TEPA ($_{2/1}$) in PBS buffer for 4 h. DAPI (4′, 6-diamidino-2-phenylindole) was used to stain the cell nuclei. High-contrast fluorescent signals from multicolored ACNDs around the nucleus of each cell established nitrogen-doped ACNDs as a useful tool for high-contrast multicolor labeling [21].

Zhang *et al*. evaluated the *in vitro* cytotoxicity of C-dots in CT26. WT and CAL-27 cells using an MTT assay. The diagnostic and cellular imaging potential of C-dots were evaluated by incubating both cell lines in 0.1–1 mg ml^{-1} solutions for 24 h. Cell viability after 24 h was found to be >82% for CT26.WT cells and >60% for CAL-27 cells at a concentration of 1 mg ml^{-1} [22].

Fu *et al*. fabricated arginine-modified C-dots (Arg-C-dots) and evaluated their *in vitro* cytotoxicity on NIH 3T3, HEK 293, HeLa, and MCF-7 cells by adding Arg-C-dots into cell media for 30 min–24 h. The authors reported 95.1, 92.4, 97.6, and 95.6% cell viability, respectively [64].

TABLE 4

***In vitro* and *in vivo* toxicity studies of C-dots**

Fabrication approach	Carbon source	Size of C-dots	Surface engineering	Cell line/animal model	Observation	Refs
In vitro toxicity studies						
Laser ablation	^{13}C powder and graphite cement	4–5 nm	PEG-1500N	MCF 7 cell	Increased cell viability	[30]
Hydrothermal treatment	PEG	2–4 nm	–	Hep G_2 cells	At 100 Mg ml^{-1} – 90% cell viability; at 400 Mg ml^{-1}, 49% cell viability	[62]
			Pyridinic-*N*, pyrollic-*N*	U-87 MG brain cells		[21]
	Citric acid and EDA	1–4.5 nm	–	NIH 3T3 cells, HEK 293 cells, HeLa cells, and MCF-7 cells	At 0.25 mg mL^{-1}, cell viability of 95% (NIH 3T3 cells), 92.4% (HEK293 cells), 97.6% (HeLa cells), and 95.9% (MCF 7 cells)	[64]
Hydrothermal carbonization	Linear PEI and citric acid		PEA analog, EDA, DETA, TEPA	HeLa cells	At 800 Mg ml^{-1}, 90% cell viability	[21]
Heat reflux method	L-glutamic acid	5.42 nm	PEG 200	CT26WT and CAL-27T cells	At 0.1–1 mg ml^{-1}, cell viability of 82% (CT26WT cells) and 60% (CAL-27T cells)	[22]
Polymerization approach	α-cyclodextrin	70–80 nm	HPG using grafting method	A549 cells	At 0.1 mg ml^{-1}, cell viability >90%	[65]
***In vivo* toxicity studies**						
Laser ablation	^{13}C powder and graphite cement	4–5 nm	PEG 1500 N	Mice	Post 24 h, low accumulation; post 28 days, no detectable chemical symptoms	[30]
Mixed acid treatment	SWCNTs, MWCNTs, and graphite	3–4 nm		Mice	No toxic effects, weight loss, or death of mice	[67]
Nitric acid oxidation	Raw soot	1–3 nm	PEG 2000N	Mice	No abnormality or gene toxicity	[68]

Li *et al*. fabricated C-dot-based nanohybrids with multihydroxy hyperbranched polyglycerol (HPG) using a grafting form method and performed cytotoxic evaluations at concentrations of 0.1–10 mg ml^{-1}. The HPG-C-dots nanohybrids reported lower cytotoxicity compared with the C-dots, with a cell viability >90% at a concentration of 0.1 mg ml^{-1} [65].

In vivo *toxicity studies*

Functional group passivation affects the toxicity of C-dots. PEG-modified C-dots were found to be nontoxic and, thus, could be used for imaging and other applications [66]. Although *in vitro* studies have reported the nontoxic nature of luminescent C-dots, few data are available from *in vivo* toxicity studies.

Yang *et al*. demonstrated the nontoxic nature of C-dots *in vivo* following intravenous administration in mice. The C-dots were found in the liver, kidney, and spleen, and showed noneffective toxicity, little accumulation of C-dots, and renal clearance within 24 h. No chemical symptoms were detected after 28 days [30].

Tao *et al*. injected 20 mg/kg C-dots into mice and carried out a 3-month continuous investigation. Given their nontoxic nature, neither weight loss nor any mortality was observed [67]. In another study, Wang *et al*. reported the low *in vivo* toxicity of C-dots fabricated from raw soot by nitric acid treatment and PEG passivation. In the study, C-dots were evaluated gradually for acute toxicity, subacute toxicity, and genotoxicity. Experiments involved mouse bone marrow micronuclear tests and *Salmonella typhimurium* mutagenicity tests. The results demonstrated no abnormality, no obvious toxic effects in the organs of the mice, and no gene toxicity [68].

Remedies for reducing toxicity

Molecules, such as polyacrylic acid (PAA) and branched polyethylenimine (BPEI), have relatively higher toxicity compared with other molecules. In the case of PAA-functionalized C-dots, free PAA is toxic to cells if their exposure period is >24 h. The remedy for such toxicity is to shorten the incubation time, and use a minimum concentration and surface engineering. The toxicity decreased with a reduction in exposure time to 4 h [3]. Although C-dots are nontoxic, their toxicity can be further reduced by surface-engineering techniques that use biocompatible polymers, such as PEG (PEGylation) and amino acids.

Carbon dots in targeted drug delivery

C-dots are excellent drug delivery tools because of their particle size, simple fabrication and purification techniques, sustained drug release, biocompatibility, lower cytotoxicity, and other properties [31]. C-dots overcome the minimum observability and traceability problem of conventional drug carriers. Fluorescent C-dots are used as drug carrier moieties because of their modified functional groups, low cytotoxicity, and maximum drug-loading capacity [2].

Zheng and co-workers passivated the amino group on the surface of C-dots with oxaliplatin (Oxa-C-dots) by a chemical coupling reaction, which coupled the optical properties of C-dots

and the therapeutic performance of Oxa. *In vitro* studies demonstrated that Oxa-C-dots had anticancer effects and bioimaging functions, with good biocompatibility. *In vivo* results demonstrated that drug distribution by Oxa-C-dots could be traced by monitoring the fluorescence signal, which could aid in dose and injection time customization of such medication. Modified Oxa-C-dots changed the internal environment of cancer cells and entered by endocytosis. The distribution of Oxa in cancer cells could be detected because of the fluorescent nature of the C-dots [69].

Lai *et al*. worked on drug delivery using C-dots and obtained excellent optical properties of C-dots by conjugating $mSiO_2$-PEG to the surface of the dots. The $mSiO_2$-PEG-C-dots were used as a drug carrier for the anticancer drug DOX in HeLa cells [11].

Wang *et al*. studied luminescent hollow C-dots and reported their advantages as a drug delivery tool. Hollow C-dots at a concentration <100 mg/ml were reported to be biocompatible. Additionally, DOX and DOX-C-dots exhibited similar cytotoxicity profiles. The pharmacodynamic activity of DOX was not affected by the C-dots. Fluorescence imaging showed internalization of the DOX-loaded C-dots, with green fluorescence reported under blue illumination. In the cell nuclei, red fluorescence confirmed the absence of C-dots and complete release of drug from the dots [68].

Tang *et al*. reported a surface-engineered Forster resonance energy transfer (FRET)-based C-dot drug delivery system (FRET-C-dots-DDS), which facilitated real-time monitoring of drug release profile and cellular imaging depending on the FRET signal. The delicate interaction between the fluorescent nanomaterial probe and guest drug molecule showed the separation between accepter and donor affecting the FRET signal. In the developed drug delivery system, C-dots performed a dual role as a FRET pair donor without the use of extra fluorescent labeling, and as a drug carrier moiety. This FRET-based drug delivery system showed high drug release efficiency towards cancer cells. For targeting cancerous cells, folic acid (FA) was combined with PEGylated C-dots. A correlation between energy transfer from the C-dots to DOX and intrinsic emission were observed. As the DOX molecule released from C-dots surface, the FRET signal was detected at 498 nm [70].

In another study, Mewada *et al*. fabricated C-dots from sorbitol and further passivated them with bovine serum albumin (BSA), which improved the drug-loading capacity and biocompatibility. DOX was loaded on the surface of BSA-C-dots with an 86% drug-loading capacity. At pH 7.2, this complex displayed 12% drug release. The BSA-C-dots killed more cancer cells than did the free BSA [71].

Recently, Wang *et al*. reported C-dots fabricated from Tsingtao® beer as an efficient nanocarrier for cancer treatment. DOX-conjugated beer C-dots (BC-dots) exerted a prolonged drug release profile towards MCF-7 cells. Laser scanning confocal microscopy confirmed the internalization of BC-dots-DOX in MCF-7 cells. *In vitro* analysis of BC-dots-DDS showed bioimaging function and anticancer activity with excellent biocompatibility [21].

Feng *et al*. developed tumor extracellular microenvironment-responsive nanocarriers comprising cisplatin (intravenous) and drug-loaded charge-convertible C-dots. *In vitro* studies confirmed the better therapeutic efficiency of the charge-convertible nanocarriers in a tumor extracellular environment, which also confirmed its efficiency to be better than that of noncharge-convertible nanocarriers under normal physiological conditions [72].

Recently, Zhang *et al*. fabricated pH triggered-multifunctional DDS using DOX hydrochloride, N-doped C-dots, and heparin (Hep). DOX and Hep were attached to C-dots via chemical bonds. The Hep/DOX-C-dots DDS displayed good stability with a pH-responsive accelerated release rate of Hep and DOX in an acidic buffer [57].

Recently, Shu *et al*. constructed a drug delivery system by combining ion liquid-mediated organophilic C-dots (IL-OC-dots) and curcumin (Cur), an anticancer drug, using hydrophobic interactions, and reported 1,3-dibutylimidazolium nitrate-derived IL-OC-dots to be efficient drug carriers, with a rapid cell-penetrating potential of Cur and high drug-loading capacity, which facilitated the apoptosis of HeLa cells. An organophilic carrier was selected for drug loading and drug delivery because of the hydrophobic nature of C-dots. The authors reported 69.2% drug loading and 87.5% HeLa cell viability at 20 mg ml^{-1} of IL-OC-dots. These results clearly showed that IL-OC-dots-Cur-DDS enhanced the drug penetration into cells and resulted in the death of cancer cells [73].

Surface functional moieties grafted onto the surface of C-dots render them potential candidates in targeted drug delivery. Until recently, there was a lack of an all-round multifunctional agent that could perform cellular imaging, drug targeting, and therapeutic functions simultaneously. The nontoxic nature of C-dots renders them useful for all such functions.

Zheng and co-workers fabricated fluorescent self-targeting C-dots for the diagnosis of cancerous brain cells by selecting D-glucose (Glu) and L-aspartic acid (Asp) as starting materials using thermolysis breakdown. The authors reported bright fluorescence upon targeting glioma cells and penetrating the blood–brain barrier (BBB). During *in vivo* studies, the high-contrast biodistribution of Asp-C-dots was observed 15 min after injection of the Asp-C-dots through the tails of the mice. This showed that Asp-C-dots performed the dual functions of targeting and bioimaging in C6 glaucoma cells [74].

Jung *et al*. pioneered a nucleus-targeted drug delivery system using zwitterionic C-dots for anticancer therapy. The authors used β-alanine as the passivating agent for facilitating cytoplasmic uptake and zwitterionic ligands for successive nuclear translocation using a one-step fabrication technique. The targeted drug delivery system was formed by grafting DOX on the surface of the C-dots, which increased their nuclear delivery and accumulation in tumors *in vitro* and *in vivo,* respectively. Efficient translocation within the nucleus and high biocompatibility increased the nuclear drug uptake [75].

Recently, Yang *et al*. developed nuclear localization single-peptide-based C-dots (NLS-C-dots) for DOX delivery in tumor cells and studied apoptosis in human lung adenocarcinoma A549 cell lines. Acid-liable hydrazine bonds were used to couple DOX to the NLS-C-dots. Fluorescent imaging showed the presence of DOX NLS-C-dots within the nucleus. The results showed the improved ability of DOX NLS-C-dots to kill cancerous cell compared with free DOX [76].

To promote the clinical prospectives of C-dots in cancer therapeutics, Zheng *et al*. developed green-emitting C-dots by conjugating the amine group of DOX and carboxyl moiety present on the surface of C-dots via non-covalent bonding [77]. Feng *et al*.

developed dual-responsive C-dots for enhanced anticancer drug delivery and tumor extracellular microenvironment-triggered targeting. The drug delivery system, comprising cisplatin (IV) as the prodrug, C-dots as the drug carrier and RGD ligands for active targeting, was enclosed by monomethoxy polyethylene glycol (mPEG). The inner targeting of the RGD peptide was exposed following hydrolysis of the benzoic-imine bond at a tumor extracellular pH (6.5–6.8). The multicolor fluorescence of C-dots accompanied drug nanocarriers via RGD-integrin $\alpha v\beta_3$ and displayed the effective uptake of the drug nanocarrier by the cancer cells [72].

Recently, Singh *et al*. fabricated DNA-C-dots by attaching amine-functionalized C-dots to the 5′-phosphate termini of a cytosine-rich single-stranded DNA phosphoramidate linkage for sustained and targeted drug release. DOX was loaded onto a hydrogel, which acted as a reservoir for sustained drug release. In this drug delivery system, C-dots had a dual role as cross-linkers for network formation and for encapsulation of the drug via electrostatic interactions with DNA [78].

Carbon dots in gene delivery

Gene therapy, a promising option for the treatment of many diseases, requires a safe and efficient carrier for the delivery of fluorescent and biocompatible therapeutic payloads. The properties of C-dots make them efficient emerging carriers for gene delivery. Liu and co-workers utilized PEI (bPEI25K) passivated C-dots as transfection agents. The results showed bright fluorescence and excellent water solubility with low cytotoxicity and efficient *in vitro* DNA transfection [38]. Kim *et al*. performed *in vitro* DNA transfection and monitored the cellular plasmid trafficking. The authors compared the use of PEI-functionalized C-dots (PEI-C-dots), PEI-functionalized gold colloids (PEI-AU), and plasmid DNA (pDNA) for gene delivery The initial connection of PEI-C-dots with PEI-AU showed weak fluorescence during transfection. With a relatively high concentration, pDNA and high fluorescence were reported by dissociation of PEI-C-dots from PEI-AU, thus facilitating gene delivery and the monitoring of cellular trafficking [79].

Recently, Zhang *et al*. developed hyaluronic acid (HA)/PEI functionalized C-dots (HP-C-dots) using a bottom-up approach for tumor targeting and gene therapy. The HP-C-dots showing good biocompatibility, excellent gene condensation capacity, and water dispersibility, and were readily internalized into cancer cells via HA-receptor-mediated endocytosis. The resultant HP-C-dots proved to be potential candidates for tumor targeting and gene delivery [57].

Carbon dots in diagnostic imaging

Diagnostic imaging is necessary for diagnosing diseases *in vivo* and for targeted drug delivery. For diagnostic *in vitro* and *in vivo* imaging, fluorescent NPs are basic units for determining the applicability of NPs as imaging probes. The cytotoxicity of NPs has an important role in diagnostic imaging. However, environmental issues arising from the use of semiconducting Q-dots, such as CdSe and other compounds, limit their imaging applications. By contrast, C-dots are emerging candidates as diagnostic imaging probes because of their prominent biocompatibility, low cytotoxicity, nanosize, excellent photostability, and multicolor emissions.

Zhai *et al*. fabricated photoluminescent C-dots to label L929 cells at λ_{ex} 405, 488, and 543 nm. EDA-C-dots emitted blue, green, and red fluorescence, respectively. Cellular areas reflecting the emitted fluorescence indicated the presence of C-dots. C-dots were reported mainly around the cell nucleus and in the cytoplasm and cell membrane [80].

Wu *et al*. performed *in vivo* photoacoustic (PA) imaging of sentinel lymph nodes (SLN) using passivated C-dots. The imaging probes gave strong observable optical absorption signals in the near-infrared (NIR) region after 2 min. Faster resection of SLN occurred because of the small size of the probe and rapid lymphatic transport, overcoming the issues associated with the use of dyes [12].

In another study, Kasibabu *et al*. synthesized C-dots from *Punicagrantum* fruits as imaging probes for bacterial and fungal cells. These C-dots exhibited no cytotoxic effects and inhibited the growth of *Bacillus subtilis*. Thus, C-dots could also be used for imaging of animal and plant cells [81].

Ge *et al*. designed C-dots by hydrothermal treatment of polythiophene phenyl propionic acid (PPA) for propionic acid imaging, which resulted in a broad absorption spectrum in the NIR region. In addition, under NIR light irradiation, C-dots displayed high photothermal conversion efficiency. Laser photothermal ablation of xenografted tumor in mice was achieved at 671 nm [82].

In another study, C-dots showed fluorescence imaging in zebrafish embryos. More than 80% and 55% embryo or larval viability was reported with C-dots at a concentration of 1.25 and 2.5 mg ml^{-1}, respectively. This illustrated the high biocompatibility and lower toxic nature of C-dots [83].

Jiang *et al*. selected three isomers of phenylenediamines, namely, o-, m-, and p-phenylenediamines, to fabricate C-dots by facile solvothermal treatment. Incubating these three C-dots with MCF-7 cells for 4 h followed by further laser excitation at 405 nm resulted in the cells exhibiting different-colored emissions [45].

Wang *et al*. also performed a systematic *in vitro* and *in vivo* bioimaging study using high-performance photoluminescent C-dots. Fluorescence signals were observed at 535 nm and 695–770 nm following subsequent injections of 0.5 and 5 mg C-dots, respectively, into athymic BALB/C-nu mice. Better penetration ability of C-dots compared with visible light reflected their potential for use in *in vivo* imaging (Fig. 5) [21].

Li *et al*. fabricated N,P-C-dots by microwave-assisted thermolysis of *N*-phosphonomethylaminodiacetic acid and EDA. With an emission at 418 nm, N,P-C-dots exhibited bright-blue fluorescence. Uniform dispersion of N,P-C-dots with an average size of 3.3 nm, 17.5% QY, good stability, and low toxicity indicated their successful use as a fluorescent nanomaterial probe for cellular imaging [84].

Recently, Parvin and Mandal fabricated P,N-C-dots using hydrothermal treatment of a mixture of phosphoric acid (PA), EDA, and citric acid. C-dots find applications in PA imaging and fluorescent imaging of living tissue because of their wavelength-dependent emission, insensitivity to pH changes, C-dot concentration, green fluorescence at 430 nm with 30% QY, and red fluorescence at 500 nm with 78% QY, with improved spatial resolution and deeper tissue imaging [85].

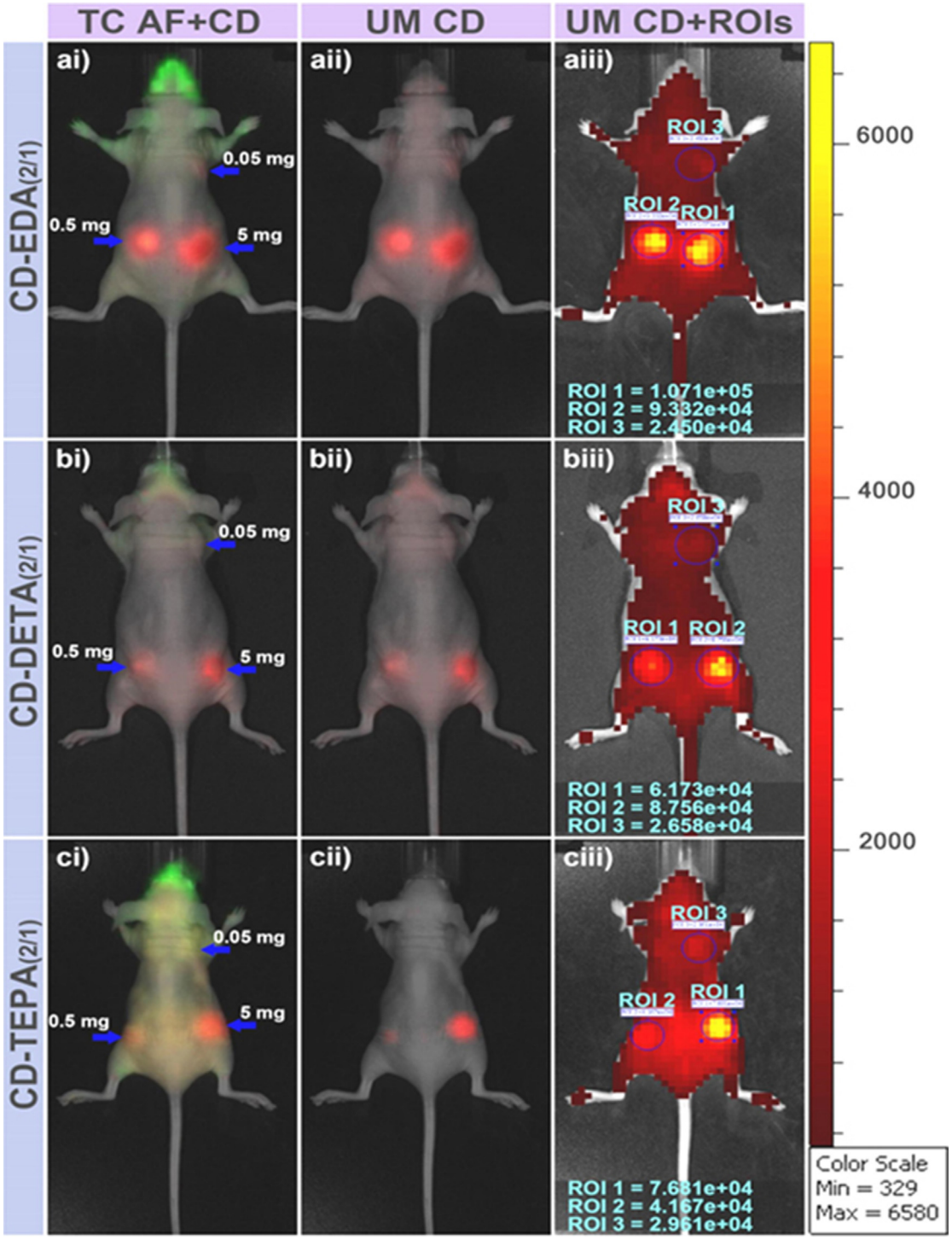

FIGURE 5

In vivo fluorescence imaging of nude mice injected subcutaneously with carbon quantum dot (CQD)-1,2-ethylenediamine (EDA) $_{(2/1)}$, CQD-diethylenetriamine (DETA) $_{(2/1)}$, and CQD-tetraethylenepentamine (TEPA) $_{(2/1)}$ at three injection sites (blue arrow) with increased doses (ai, bi, ci). The true color (TC) fluorescent composite images of CQD fluorescence and autofluorescence (AF) from mice (aii, bii, cii), unmixed (UM) images of CQD fluorescence (aiii, biii, ciii). Fluorescent intensities measured in region of interest (ROI). Reproduced, with permission, from Ref. [61].

Concluding remarks and future perspectives

As per previously published reports, C-dots can be exploited as outstanding drug delivery tools because of their specific properties, including high drug-loading capacity, simple fabrication techniques, and nanometric sizes. On grafting with an anticancer drug, C-dots demonstrated their biocompatibility against normal cells and toxicity towards cancer cells, while simultaneously performing theranostic roles. Here, we have summarized recent advances in the use of natural and synthetic fabrication techniques of C-dots along with their development into an emerging nanoarchitecture for targeted drug delivery and bioimaging. Physicochemical properties, such as photoluminescence and fluorescence, which affect their bioapplications have been discussed, as well as their advantages and disadvantages. The

excitation-dependent and independent properties of C-dots demonstrate that their structure-specific properties s can be fine-tuned by surface engineering. *In vitro* and *in vivo* studies have also highlighted the low or nontoxic nature of C-dots compared with other nanomaterials.

C-dots have resolved the problems of tracing and observing conventional drug carriers. Incorporation of one or more functional moieties onto the surface of C-dots could be a useful tool for the treatment of disease. In addition, the issue of healthy tissues being damaged by conventional chemotherapy can also be resolved by C-dots.

Although C-dots are thought to have more-efficient nanoarchitectures for drug delivery and bioimaging, there are some problems associated with their use, including poor control over their size and surface properties, which impede their applications. Although much work has been done on C-dots, the origin and mechanism of their photoluminescence remain unclear because C-dots fabricated using different processes show non-uniform photoluminescence and variable sizes. Their complex composition and further purification issues limit the use of C-dots. However, future research should aim to clarify the applications of C-dots. In addition, studies of newer fabrication techniques with high QY as well as of the origin and mechanism of photoluminescence are desirable. Nevertheless, it is likely that C-dots will improve human healthcare in the future via their use for targeted drug delivery and diagnostic imaging.

References

1 Resch-Genger, U. *et al.* (2008) Quantum dots versus organic dyes as fluorescent labels. *Nat. Methods* 5, 763–775
2 Zuo, J. *et al.* (2015) Preparation and application of fluorescent carbon dots. *J. Nanomater.* 2015, 1–13
3 Wang, Y. and Hu, A. (2014) Carbon quantum dots: synthesis, properties and applications. *J. Mater. Chem. C* 2, 6921–6939
4 Yang, Z.C. *et al.* (2011) Intrinsically fluorescent carbon dots with tunable emission derived from hydrothermal treatment of glucose in the presence of monopotassium phosphate. *Chem. Commun.* 47, 11615–11617
5 Sk, M.P. *et al.* (2012) Presence of amorphous carbon nanoparticles in food caramels. *Sci. Rep.* 2, 383
6 Liu, S. *et al.* (2012) Hydrothermal treatment of grass: a low-cost, green route to nitrogen-doped, carbon-rich, photoluminescent polymer nanodots as an effective fluorescent sensing platform for label-free detection of Cu(II) ions. *Adv. Mater.* 24, 2037–2041
7 Wang, J. *et al.* (2012) Amphiphilic egg-derived carbon dots: rapid plasma fabrication, pyrolysis process, and multicolor printing patterns. *Angew. Chem. Int. Ed. Engl.* 51, 9297–9301
8 Zhu, C. *et al.* (2012) Bifunctional fluorescent carbon nanodots: green synthesis via soy milk and application as metal-free electrocatalysts for oxygen reduction. *Chem. Commun.* 48, 9367–9369
9 Liao, H. *et al.* (2015) Fluorescent nanoparticles from several commercial beverages: their properties and potential application for bioimaging. *J. Agric. Food Chem.* 63, 8527–8533
10 Sahu, S. *et al.* (2012) Simple one-step synthesis of highly luminescent carbon dots from orange juice: application as excellent bio-imaging agents. *Chem. Commun.* 48, 8835–8837
11 Lai, C.-W. *et al.* (2012) Facile synthesis of highly emissive carbon dots from pyrolysis of glycerol; gram scale production of carbon dots/$mSiO_2$ for cell imaging and drug release. *J. Mater. Chem.* 22, 14403–14409
12 Wu, Z.L. *et al.* (2013) One-pot hydrothermal synthesis of highly luminescent nitrogen-doped amphoteric carbon dots for bioimaging from Bombyx mori silk – natural proteins. *J. Mater. Chem. B* 1, 2868–2873
13 Jahan, S. *et al.* (2013) Oxidative synthesis of highly fluorescent boron/nitrogen co-doped carbon nanodots enabling detection of photosensitizer and carcinogenic dye. *Anal. Chem.* 85, 10232–10239
14 Chen, Q.-L. *et al.* (2013) One-step synthesis of yellow-emitting carbogenic dots toward white light-emitting diodes. *J. Mater. Sci.* 48, 2352–2357
15 De, B. and Karak, N. (2013) A green and facile approach for the synthesis of water soluble fluorescent carbon dots from banana juice. *RSC Adv.* 3, 8286–8290
16 Dong, Y. *et al.* (2013) Carbon-based dots co-doped with nitrogen and sulfur for high quantum yield and excitation-independent emission. *Angew. Chem. Int. Ed. Engl.* 52, 7800–7804
17 Xu, Z.-Q. *et al.* (2014) Low temperature synthesis of highly stable phosphate functionalized two color carbon nanodots and their application in cell imaging. *Carbon* 66, 351–360
18 Yang, S. *et al.* (2014) Large-scale fabrication of heavy doped carbon quantum dots with tunable-photoluminescence and sensitive fluorescence detection. *J. Mater. Chem. A* 2, 8660–8667
19 Jiang, C. *et al.* (2014) Presence of photoluminescent carbon dots in Nescafe® original instant coffee: Applications to bioimaging. *Talanta* 127, 68–74
20 Xu, J. *et al.* (2015) Carbon dots as a luminescence sensor for ultrasensitive detection of phosphate and their bioimaging properties. *Luminescence* 30, 411–415
21 Wang, Z. *et al.* (2015) Fluorescent carbon dots from beer for breast cancer cell imaging and drug delivery. *Anal. Methods* 7, 8911–8917
22 Zhang, J. and Yu, S.-H. (2016) Carbon dots: large-scale synthesis, sensing and bioimaging. *Mater. Today* 19, 382–393
23 Ramanan, V. *et al.* (2016) Outright green synthesis of fluorescent carbon dots from eutrophic algal blooms for *in vitro* imaging. *ACS Sustain. Chem. Eng.* 4, 4724–4731
24 Xu, X. *et al.* (2004) Electrophoretic analysis and purification of fluorescent single-walled carbon nanotube fragments. *J. Am. Chem. Soc.* 126, 12736–12737
25 Zhu, H. *et al.* (2009) Microwave synthesis of fluorescent carbon nanoparticles with electrochemiluminescence properties. *Chem. Commun.* 34, 5118–5120
26 Li, X. *et al.* (2010) Preparation of carbon quantum dots with tunable photoluminescence by rapid laser passivation in ordinary organic solvents. *Chem. Commun.* 47, 932–934
27 Li, H. *et al.* (2011) Fluorescent carbon nanoparticles: electrochemical synthesis and their pH sensitive photoluminescence properties. *New J. Chem.* 35, 2666–2670
28 Liu, W. *et al.* (2016) Carbon dots: surface engineering and applications. *J. Mater. Chem. B* 4, 5772–5788
29 Zeni, O. *et al.* (2008) Cytotoxicity investigation on cultured human blood cells treated with single-wall carbon nanotubes. *Sensors* 8, 488–499
30 Yang, S.T. *et al.* (2009) Carbon dots as nontoxic and high-performance fluorescence imaging agents. *J. Phys. Chem. C Nanomater. Interfaces* 113, 18110–18114
31 Ashmi, M. (2014) Swarming carbon dots for folic acid mediated delivery of doxorubicin and biological imaging. *J. Mater. Chem. B* 2, 698–705
32 Wang, J. and Qiu, J. (2016) A review of carbon dots in biological applications. *J. Mater. Sci.* 51, 4728–4738
33 Kroto, H.W. *et al.* (1985) C_{60}: buckminsterfullerene. *Nature* 318, 162–163
34 Dresselhaus, M.S. and Avouris, P. (2001) Introduction to carbon materials research. *Carbon Nanotubes* 80, 1–9
35 Sun, Y.P. *et al.* (2006) Quantum-sized carbon dots for bright and colorful photoluminescence. *J. Am. Chem. Soc.* 128, 7756–7757
36 Park, S.Y. *et al.* (2014) Photoluminescent green carbon nanodots from food-waste-derived sources: large-scale synthesis, properties, and biomedical applications. *ACS Appl. Mater. Interfaces* 6, 3365–3370
37 Hu, S.-L. *et al.* (2009) One-step synthesis of fluorescent carbon nanoparticles by laser irradiation. *J. Mater. Chem.* 19, 484–488
38 Liu, C. *et al.* (2012) Nano-carrier for gene delivery and bioimaging based on carbon dots with PEI-passivation enhanced fluorescence. *Biomaterials* 33, 3604–3613
39 Roy, P. *et al.* (2015) Photoluminescent carbon nanodots: synthesis, physicochemical properties and analytical applications. *Mater. Today* 18, 447–458
40 Zhang, Y.-Y. *et al.* (2013) A new hydrothermal refluxing route to strong fluorescent carbon dots and its application as fluorescent imaging agent. *Talanta* 117, 196–202
41 Deng, Y. *et al.* (2013) Long lifetime pure organic phosphorescence based on water soluble carbon dots. *Chem. Commun.* 49, 5751–5753
42 Lin, Z. *et al.* (2012) Classical oxidant induced chemiluminescence of fluorescent carbon dots. *Chem. Commun.* 48, 1051–1053
43 Zhao, L. *et al.* (2013) Chemiluminescence of carbon dots under strong alkaline solutions: a novel insight into carbon dot optical properties. *Nanoscale* 5, 2655–2658
44 Liao, B. *et al.* (2014) Synthesis of fluorescent carbon nanoparticles grafted with polystyrene and their fluorescent fibers processed by electrospinning. *RSC Adv.* 4, 57683–57690

45 Jiang, K. *et al.* (2015) Red, green, and blue luminescence by carbon dots: full-color emission tuning and multicolor cellular imaging. *Angew. Chem. Int. Ed.* 54, 5360–5363

46 Wang, R. *et al.* (2017) One-step synthesis of self-doped carbon dots with highly photoluminescence as multifunctional biosensors for detection of iron ions and pH. *Sens. Actuators B Chem.* 241, 73–79

47 Li, L. *et al.* (2015) Nitrogen and sulfur co-doped carbon dots for highly selective and sensitive detection of Hg (II) ions. *Biosens. Bioelectron.* 74, 263–269

48 Zhuo, Y. *et al.* (2015) One-step synthesis of high quantum-yield and excitation-independent emission carbon dots for cell imaging. *Mater. Lett.* 139, 197–200

49 Himaja, A. *et al.* (2015) Carbon dots: the newest member of the carbon nanomaterials family. *Chem. Rec.* 15, 595–615

50 Hsu, P.-C. *et al.* (2012) Synthesis and analytical applications of photoluminescent carbon nanodots. *Green Chem.* 14, 917–920

51 Peng, H. and Travas-Sejdic, J. (2009) Simple aqueous solution route to luminescent carbogenic dots from carbohydrates. *Chem. Mater.* 21, 5563–5565

52 Zhou, J.-H. *et al.* (2007) CTAB assisted microwave synthesis of ordered mesoporous carbon supported Pt nanoparticles for hydrogen electro-oxidation. *Electrochim. Acta* 52, 4691–4695

53 Bhunia, S.K. *et al.* (2013) Carbon nanoparticle-based fluorescent bioimaging probes. *Sci. Rep.* 3, 1473

54 Dong, X. *et al.* (2010) Electrical detection of DNA hybridization with single base specificity using transistors based on CVD grown graphene sheets. *Adv. Mater.* 22, 1649–1653

55 Du, F. *et al.* (2013) Carbon dots-based fluorescent probes for sensitive and selective detection of iodide. *Microchim. Acta* 180, 453–460

56 Liu, Y. *et al.* (2014) One-step microwave-assisted polyol synthesis of green luminescent carbon dots as optical nanoprobes. *Carbon* 68, 258–264

57 Zhang, M. *et al.* (2017) Fabrication of HA/PEI-functionalized carbon dots for tumor targeting, intracellular imaging and gene delivery. *RSC Adv.* 7, 3369–3375

58 Ming, H. *et al.* (2012) Large scale electrochemical synthesis of high quality carbon nanodots and their photocatalytic property. *Dalton Trans.* 41, 9526–9531

59 Deng, J. *et al.* (2014) Electrochemical synthesis of carbon nanodots directly from alcohols. *Chemistry* 20, 4993–4999

60 Kong, B. *et al.* (2012) Carbon dot-based inorganic–organic nanosystem for two-photon imaging and biosensing of pH variation in living cells and tissues. *Adv. Mater.* 24, 5844–5848

61 Li, X. *et al.* (2014) Engineering surface states of carbon dots to achieve controllable luminescence for solid–luminescent composites and sensitive Be^{2+} detection. *Sci. Rep.* 4, 4976

62 Fan, R.-J. *et al.* (2014) Photoluminescent carbon dots directly derived from polyethylene glycol and their application for cellular imaging. *Carbon* 71, 87–93

63 Zhao, Q.-L. *et al.* (2008) Facile preparation of low cytotoxicity fluorescent carbon nanocrystals by electrooxidation of graphite. *Chem. Commun.* 41, 5116–5118

64 Fu, H. *et al.* (2017) A versatile ratiometric nanosensing approach for sensitive and accurate detection of Hg^{2+} and biological thiols based on new fluorescent carbon quantum dots. *Anal. Bioanal. Chem.* 409, 2373–2382

65 Li, S. *et al.* (2017) Hyperbranched polyglycerol conjugated fluorescent carbon dots with improved *in vitro* toxicity and red blood cell compatibility for bioimaging. *RSC Adv.* 7, 4975–4982

66 Wang, Y. *et al.* (2011) Carbon dots of different composition and surface functionalization: cytotoxicity issues relevant to fluorescence cell imaging. *Exp. Biol. Med.* 236, 1231–1238

67 Tao, H. *et al.* (2012) *In vivo* NIR fluorescence imaging, biodistribution, and toxicology of photoluminescent carbon dots produced from carbon nanotubes and graphite. *Small* 8, 281–290

68 Wang, K. *et al.* (2013) Systematic safety evaluation on photoluminescent carbon dots. *Nanoscale Res. Lett.* 8, 122

69 Zheng, M. *et al.* (2014) Integrating oxaliplatin with highly luminescent carbon dots: an unprecedented theranostic agent for personalized medicine. *Adv. Mater.* 26, 3554–3560

70 Tang, J. *et al.* (2013) Carbon nanodots featuring efficient FRET for real-time monitoring of drug delivery and two-photon imaging. *Adv. Mater.* 25, 6569–6574

71 Mewada, A. *et al.* (2014) Swarming carbon dots for folic acid mediated delivery of doxorubicin and biological imaging. *J. Mater. Chem. B* 2, 698–705

72 Feng, T. *et al.* (2016) Charge-convertible carbon dots for imaging-guided drug delivery with enhanced *in vivo* cancer therapeutic efficiency. *ACS Nano* 10, 4410–4420

73 Shu, Y. *et al.* (2017) Ionic liquid mediated organophilic carbon dots for drug delivery and bioimaging. *Carbon* 114, 324–333

74 Zheng, M. *et al.* (2015) Self-targeting fluorescent carbon dots for diagnosis of brain cancer cells. *ACS Nano* 9, 11455–11461

75 Jung, Y.K. *et al.* (2015) Cell nucleus-targeting zwitterionic carbon dots. *Sci. Rep.* 5, 18807

76 Yang, L. *et al.* (2016) Doxorubicin conjugated functionalizable carbon dots for nucleus targeted delivery and enhanced therapeutic efficacy. *Nanoscale* 8, 6801–6809

77 Zeng, Q. *et al.* (2016) Carbon dots as a trackable drug delivery carrier for localized cancer therapy *in vivo*. *J. Mater. Chem. B* 4, 5119–5126

78 Singh, S. *et al.* (2017) Carbon dots assisted formation of DNA hydrogel for sustained release of drug. *Carbon* 114, 169–176

79 Kim, J. *et al.* (2013) Transfection and intracellular trafficking properties of carbon dot-gold nanoparticle molecular assembly conjugated with PEI-pDNA. *Biomaterials* 34, 7168–7180

80 Zhai, X. *et al.* (2012) Highly luminescent carbon nanodots by microwave-assisted pyrolysis. *Chem. Commun.* 48, 7955–7957

81 Kasibabu, B.S.B. *et al.* (2015) One-step synthesis of fluorescent carbon dots for imaging bacterial and fungal cells. *Anal. Methods* 7, 2373–2378

82 Ge, J. *et al.* (2015) Red-emissive carbon dots for fluorescent, photoacoustic, and thermal theranostics in living mice. *Adv. Mater.* 27, 4169–4177

83 Kang, Y.-F. *et al.* (2015) Carbon quantum dots for zebrafish fluorescence imaging. *Sci. Rep.* 5, 11835

84 Li, H. *et al.* (2016) Microwave-assisted synthesis of N, P-doped carbon dots for fluorescent cell imaging. *Microchim. Acta* 183, 821–826

85 Parvin, N. and Mandal, T.K. (2017) Dually emissive P, N-co-doped carbon dots for fluorescent and photoacoustic tissue imaging in living mice. *Microchim. Acta* 184, 1117–1125

86 Scida, K. *et al.* (2011) Recent applications of carbon-based nanomaterials in analytical chemistry: critical review. *Anal. Chim. Acta* 691, 6–17

87 Patil, S. *et al.* (2018) Temperature dependent electron transport properties of gold nanoparticles and composites: scanning tunneling spectroscopy investigations. *J. Nanosci. Nanotechnol.* 18, 1626–1635

88 Mishra, V. and Kesharwani, P. (2016) Dendrimer technologies for brain tumors. *Drug Discov. Today* 21, 766–778